Massive MIMO in Spectrum Sharing Networks: Achievable Rate and Power Efficiency

Lifeng Wang, Hien Quoc Ngo, *Student Member, IEEE*, Maged Elkashlan, *Member, IEEE*, Trung Q. Duong, *Senior Member, IEEE*, and Kai-Kit Wong, *Senior Member, IEEE*

***Abstract*—Massive multiple input multiple output (MIMO) is one of the key technologies for fifth generation and can substantially improve energy and spectrum efficiencies. This paper explores the potential benefits of massive MIMO in spectrum sharing networks. We consider a multiuser MIMO primary network, with $N_{\mathtt{P}}$-antenna primary base station (PBS) and K single-antenna primary users (PUs), and a multiple-input–single-output secondary network, with $N_{\mathtt{S}}$-antenna secondary base station and a single-antenna secondary user. Using the proposed model, we derive a tight closed-form expression for the lower bound on the average achievable rate, which is applicable to arbitrary system parameters. By performing large-system analysis, we examine the impact of large number of PBS antennas and large number of PUs on the secondary network. It is shown that, when $N_{\mathtt{P}}$ and K grow large, $N_{\mathtt{S}}$ must be proportional to $\ln K$ or larger, to enable successful secondary transmission. In addition, we examine the impact of imperfect channel state information on the secondary network. It is shown that the detrimental effect of channel estimation errors is significantly mitigated as $N_{\mathtt{S}}$ grows large.**

***Index Terms*—Average achievable rate, cognitive radio, imperfect channel state information (CSI), massive multiple input multiple output (MIMO), power efficiency.**

I. Introduction

MASSIVE multiple-input–multiple-output (MIMO) systems, where a base station (BS) equipped with very large (massive) antenna arrays serves many users in the same time–frequency resource, have attracted much research interest recently [1]–[4]. One of the key properties of massive MIMO is that the channels become favorable for most propagation environments. Under favorable propagation, with simple linear processing (linear precoders in the downlink and linear decoders in the uplink), the effects of interuser interference and uncorrelated noise disappear, and hence, the linear processing is nearly optimal. Owing to the multiplexing gain and the array gain, huge spectral efficiency and energy efficiency can be obtained. In addition, [5] showed that massive MIMO is a scalable technology, and with a simple power control algorithm, massive MIMO can provide uniformly good service for all users. Therefore, massive MIMO is a promising candidate technology for "fifth" generation (5G) of wireless systems.

On a parallel avenue, over the past decade, there has been a great deal of interest in the cognitive radio technology, for its ability to improve spectrum utilization [6]–[8]. Cognitive radio refers to an opportunistic utilization of the spectrum, which enables unlicensed systems using the same spectrum as the licensed systems, while avoiding contaminating the licensed systems. Typically, there are three main cognitive radio systems: interweave, overlay, and underlay cognitive radio systems [9]. In interweave cognitive radio systems, the secondary user (SU) first senses the licensed spectrum. If this spectrum is not used by the primary users (PUs), the SU will utilize this spectrum. In overlay cognitive radio systems, the SU uses the same spectrum as the PU, and the SU has to deploy sophisticated signal processing techniques to get rid of the interference inflicted on the primary system. By contrast, in underlay cognitive radio networks, the SU is allowed to use the spectrum of the PU under the condition that the interference at the PU caused by the SU is less than a predefined interference threshold [8], [10]. The underlay cognitive radio system has attracted much recent work on its performance analysis and system design due to its operational simplicity and capacity of high spectrum utilization.

Most of existing studies in the literature consider the cognitive radio systems that the transceivers deploy only few antennas. The design and analysis of cognitive radio systems with the use of very large (massive) antenna arrays at the transceivers are of particular importance, particularly in 5G wireless systems, where a very high user throughput is required. Despite its importance, there has been very little related work in the literature [11], [12]. In [11], the authors considered a cognitive radio system where both primary and secondary networks consist of one massive antenna BS and one single-antenna user. The pilot decontamination algorithm, which aims at maximizing the quality of the channel estimation for the secondary system, was proposed. A spatial interweave cognitive radio system, which consists of the multiuser massive MIMO primary and multiuser massive MIMO secondary networks, was investigated in [12]. By contrast, in our work, we

Manuscript received December 18, 2014; revised April 29, 2015; accepted June 1, 2015. This work was supported in part by the Engineering and Physical Sciences Research Council under Grant EP/M016005/1. The work of T. Q. Duong and M. Elkashlan was supported by Newton Fund Institutional Links Grant 172719890.

L. Wang and K.-K. Wong are with the Department of Electronic and Electrical Engineering, University College London, London WC1E 7JE, U.K. (e-mail: lifeng.wang@ucl.ac.uk; kai-kit.wong@ucl.ac.uk).

H. Q. Ngo is with the Department of Electrical Engineering (ISY), Linköping University, 581 83 Linköping, Sweden (e-mail: nqhien@isy.liu.se).

M. Elkashlan is with the School of Electronic Engineering and Computer Science, Queen Mary University of London, London E1 4NS, U.K. (e-mail: maged.elkashlan@qmul.ac.uk).

T. Q. Duong is with Queen's University Belfast, Belfast BT7 1NN, U.K. (e-mail: trung.q.duong@qub.ac.uk).

Digital Object Identifier 10.1109/JSYST.2015.2449289

propose and analyze the performance of an underlay cognitive radio system, which includes a multiuser massive MIMO primary network and a multiple-input–single-output secondary network. More precisely, the primary network includes a primary base station (PBS) equipped with N_{P} antennas and K single-antenna PUs, whereas the secondary network includes one N_{S}-antenna secondary base station (SBS) and one single-antenna SU. All K PUs and SU share the same time–frequency resource. We consider the downlink transmission, and both BSs use the low-complexity maximum ratio transmission (MRT) technique. We focus on the performance of the secondary system. The main contributions of this paper are summarized as follows.

i) In contrast to [7], [8], and [10], we first derive the distribution of the signal-to-interference-plus-noise ratio (SINR) for the downlink transmission in the secondary network, considering the downlink multiuser MIMO transmission in the primary network. This is a fundamental result not found in the existing literature. Then, by using Jensen's inequality, we derive a closed-form expression for a lower bound on the average achievable rate, with any finite numbers of antennas and users. Numerical results verify the tightness of our bound, particularly when the number of BS antennas is large.

ii) We examine the potential of massive MIMO to reduce the power levels, and it is shown that the use of large antenna arrays can improve power efficiency in spectrum sharing networks. We also examine the asymptotic performances where SBSs have massive antenna arrays for both cases: perfect and imperfect channel state information (CSI) knowledge. These results enable us to examine the effects of the use of massive antenna arrays at the PBS or/and the SBS on the performance of the secondary system. More precisely, we show that the secondary system works well when the number of PBS antennas is large. However, when both N_{P} and K grow large with the same rate, the performance of the secondary system will be degraded significantly. To overcome this problem, the SBS must add more antennas. The number of SBS antennas must be proportional to $\ln K$ or more. Interestingly, we show that the adverse effect of channel estimation errors can be significantly mitigated when the number of SBS antennas is large.

The notation of this paper is as follows: $\dagger$ denotes the conjugate transpose operator, $\mathcal{CN}(\mathbf{0}, \mathbf{\Lambda})$ denotes the complex Gaussian distribution with zero mean and covariance matrix $\mathbf{\Lambda}$, $\|\cdot\|$ denotes the Euclidean norm, $\mathbb{E}\{\cdot\}$ denotes the expectation operator, $\mathbf{0}_{M\times N}$ denotes the $M \times N$ zero matrix, $\mathbf{I}_M$ denotes the $M \times M$ identity matrix, $\mathrm{tr}(\cdot)$ denotes the trace, $\overset{d}{\sim}$ denotes the same distribution, and $\overset{d}{\to}$ denotes the convergence in distribution.

II. Cognitive Radio Network

We consider the downlink transmission in the underlay spectrum sharing network. As shown in Fig. 1, the multiuser

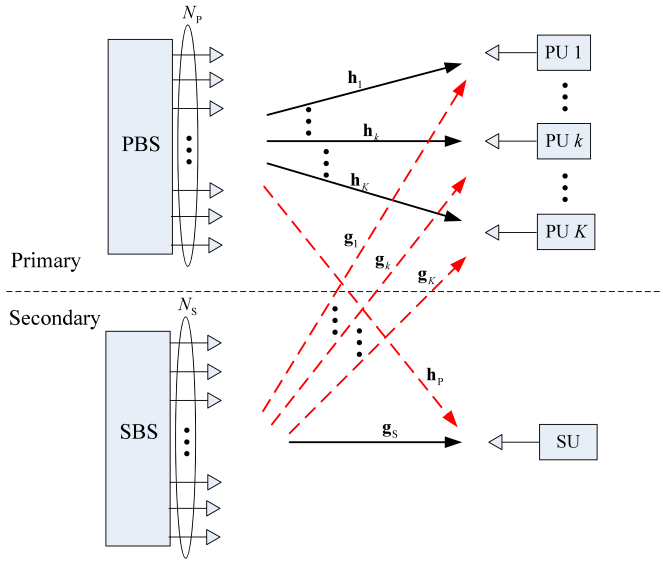

Fig. 1. Downlink transmission in the underlay spectrum sharing network.

MIMO primary network consists of a PBS equipped with N_{P} antennas and K single-antenna PUs ($N_{\mathrm{P}} \geq K$). The secondary network consists of an SBS equipped with N_{S} antennas and a SU with a single antenna. All channels are assumed to be quasi-static fading channels, where the channel coefficients are constant for each transmission block but vary independently between different blocks. In the primary network, the channel coefficient from the n_{P}th PBS antenna to the kth PU is $\sqrt{\alpha_k^{\mathrm{P}}} h_{n_{\mathrm{P}},k}$ ($n_{\mathrm{P}} = 1, \ldots, N_{\mathrm{P}}$ and $k = 1, \ldots, K$), where α_k^{P} represents the large-scale fading coefficient modeling the path loss and shadow fading and is assumed to be constant over the kth PU, and $h_{n_{\mathrm{P}},k} \sim \mathcal{CN}(0, 1)$ is the complex Gaussian random variable (RV) and represents the small-scale fading coefficient. The interfering channel coefficient from the n_{S}th SBS antenna to the kth PU is $\sqrt{\alpha_k^{\mathrm{S}}} g_{n_{\mathrm{S}},k}$ with constant value α_k^{S} and $g_{n_{\mathrm{S}},k} \sim \mathcal{CN}(0, 1)$ ($n_{\mathrm{S}} = 1, \ldots, N_{\mathrm{S}}$). In the secondary network, the channel coefficient from the n_{S}th SBS antenna to the SU is $\sqrt{\beta_{\mathrm{S}}} g_{n_{\mathrm{S}}}$ with constant value β_{S} and $g_{n_{\mathrm{S}}} \sim \mathcal{CN}(0, 1)$, and the interfering channel coefficient from the n_{P}th PBS antenna to the SU is $\sqrt{\beta_{\mathrm{P}}} h_{n_{\mathrm{P}}}$ with constant value β_{P} and $h_{n_{\mathrm{P}}} \sim \mathcal{CN}(0, 1)$.

We assume that PBS and SBS have perfect CSI, and the low-complexity MRT transmit beamformer is used at the SBS, and MRT precoding is used at the PBS. The interference power at all PUs inflicted by the SBS must not exceed the maximal peak interference level I_{P}, in order to prevent the primary transmission from harmful interference. As such, the transmit power at the SBS is given by

$$P_{\mathrm{t}} = \min\left\{\frac{I_{\mathrm{P}}}{Z_1}, P_{\mathrm{S}}\right\} \tag{1}$$

where $Z_1 = \max_k \{|\mathbf{g}_k(\mathbf{g}_{\mathrm{S}}^{\dagger}/\|\mathbf{g}_{\mathrm{S}}^{\dagger}\|)|^2\}$, $\mathbf{g}_k = \sqrt{\alpha_k^{\mathrm{S}}}[g_{1,k}, \ldots, g_{N_{\mathrm{S}},k}] \in \mathcal{C}^{1\times N_{\mathrm{S}}}$, and $\mathbf{g}_{\mathrm{S}} = \sqrt{\beta_{\mathrm{S}}}[g_1, \ldots, g_{N_{\mathrm{S}}}] \in \mathcal{C}^{1\times N_{\mathrm{S}}}$, and P_{S} is the SBS's maximum transmit power.

Given that $\mathbf{W}$ is the precoding matrix at the PBS, the received signal at the SU is

$$y = \sqrt{P_{\mathrm{t}}}\mathbf{g}_{\mathrm{S}}\frac{\mathbf{g}_{\mathrm{S}}^{\dagger}}{\|\mathbf{g}_{\mathrm{S}}^{\dagger}\|}x + \sqrt{P_{\mathrm{P}}}\mathbf{h}_{\mathrm{P}}\mathbf{W}\mathbf{z}^{T} + n_0 \tag{2}$$

where x is the transmit symbol from the SBS with $\mathbb{E}\{x\}=0$ and $\mathbb{E}\{|x|^2\}=1$; $\mathbf{z}=[z_1,\ldots,z_k,\ldots,z_K]$ is the interfering symbol vector from the PBS with $\mathbb{E}\{\mathbf{z}\}=\mathbf{0}_{1\times K}$ and $\mathbb{E}\{\mathbf{z}^{\dagger}\mathbf{z}\}=\mathbf{I}_K$; the interfering channel vector is $\mathbf{h}_{\mathrm{P}}=\sqrt{\beta_{\mathrm{P}}}[h_1,\ldots,h_{N_{\mathrm{P}}}]\in\mathcal{C}^{1\times N_{\mathrm{P}}}$; the MRT precoding matrix at the PBS is $\mathbf{W}=\sqrt{\varepsilon}\mathbf{H}$, with $\mathbf{H}=[\mathbf{h}_1^{\dagger},\ldots,\mathbf{h}_k^{\dagger},\ldots,\mathbf{h}_K^{\dagger}]\in\mathcal{C}^{N_{\mathrm{P}}\times K}$, $\mathbf{h}_k^{\dagger}=\sqrt{\alpha_k^{\mathrm{P}}}[h_{1,k},\ldots,h_{N_{\mathrm{P}},k}]^{\dagger}\in\mathcal{C}^{N_{\mathrm{P}}\times 1}$, and $\varepsilon=1/\mathbb{E}\{\mathrm{tr}(\mathbf{W}^{\dagger}\mathbf{W})\}$; P_{P} is the PBS's average transmit power; and n_0 is the additive white Gaussian noise (AWGN) with zero mean and unit variance. Based on (2), the receive SINR at the SU is given by

$$\gamma_1 = \frac{P_{\mathrm{t}}\|\mathbf{g}_{\mathrm{S}}\|^2}{\varepsilon P_{\mathrm{P}}\|\mathbf{h}_{\mathrm{P}}\mathbf{H}\|^2+1}. \tag{3}$$

In light of the SBS's transmit power P_{t} shown in (1), we reexpress (3) as

$$\gamma_1 = \frac{\min\left\{\frac{I_{\mathrm{P}}}{Z_1}, P_{\mathrm{S}}\right\}\|\mathbf{g}_{\mathrm{S}}\|^2}{\varepsilon P_{\mathrm{P}}\|\mathbf{h}_{\mathrm{P}}\mathbf{H}\|^2+1}. \tag{4}$$

III. Average Achievable Rate

Here, we derive a tight lower bound on the average achievable rate, which can be used to examine the secondary network's performance behavior. The result accurately captures the impact of arbitrary antennas and channel parameters on the average achievable rate. With this in mind, we first present some useful statistical properties in the following Proposition.

Proposition 1: The SINR of the downlink transmission from the SBS to the SU can be written as

$$\gamma_1 \overset{d}{\sim} \frac{X_1}{\varepsilon P_{\mathrm{P}} Y_1 + 1} \tag{5}$$

where $X_1=\min\{I_{\mathrm{P}}/Z_1, P_{\mathrm{S}}\}Z_2$, with $Z_2=\|\mathbf{g}_{\mathrm{S}}\|^2$, and $Y_1=\|\mathbf{h}_{\mathrm{P}}\|^2\|(\mathbf{h}_{\mathrm{P}}/\|\mathbf{h}_{\mathrm{P}}\|)\mathbf{H}\|^2=\|\mathbf{h}_{\mathrm{P}}\|^2\sum_{k=1}^{K}|\Upsilon_k|^2$, with $\Upsilon_k=(\mathbf{h}_{\mathrm{P}}/\|\mathbf{h}_{\mathrm{P}}\|)\mathbf{h}_k^{\dagger}$. The probability density function (PDF) of X_1 is given by

$$\begin{aligned} f_{X_1}(x) =& F_{Z_1}\left(\frac{I_{\mathrm{P}}}{P_{\mathrm{S}}}\right)\frac{x^{N_{\mathrm{S}}-1}e^{-\frac{x}{P_{\mathrm{S}}\beta_{\mathrm{S}}}}}{(N_{\mathrm{S}}-1)!(P_{\mathrm{S}}\beta_{\mathrm{S}})^{N_{\mathrm{S}}}} + \sum_{k=1}^{K}\frac{(-1)^{k+1}}{k!} \\ &\times \underbrace{\sum_{n_1=1}^{K}\cdots\sum_{n_k=1}^{K}}_{|n_1\bigcup\cdots\bigcup n_k|=k} \alpha^{\mathrm{S}}\frac{x^{N_{\mathrm{S}}-1}\left(\frac{x}{I_{\mathrm{P}}\beta_{\mathrm{S}}}+\alpha^{\mathrm{S}}\right)^{-(N_{\mathrm{S}}+1)}}{(N_{\mathrm{S}}-1)!(I_{\mathrm{P}}\beta_{\mathrm{S}})^{N_{\mathrm{S}}}} \\ &\times \Gamma\left(N_{\mathrm{S}}+1, \frac{x}{P_{\mathrm{S}}\beta_{\mathrm{S}}}+\frac{I_{\mathrm{P}}\alpha^{\mathrm{S}}}{P_{\mathrm{S}}}\right) \end{aligned} \tag{6}$$

where $F_{Z_1}(I_{\mathrm{P}}/P_{\mathrm{S}})=1+\sum_{k=1}^{K}((-1)^k/k!)\underbrace{\sum_{n_1=1}^{K}\cdots\sum_{n_k=1}^{K}}_{|n_1\bigcup\cdots\bigcup n_k|=k} e^{-\alpha^{\mathrm{S}}(I_{\mathrm{P}}/P_{\mathrm{S}})}$, $|n_1\bigcup\cdots\bigcup n_k|$ denotes the cardinality of the union of k indices, $\alpha^{\mathrm{S}}\triangleq(\sum_{t=1}^{k}(\alpha_{n_t}^{\mathrm{S}})^{-1})$, and $\Gamma(\cdot,\cdot)$ is the incomplete gamma function [13, (8.350.2)]. The PDF of Y_1 is given by

$$\begin{aligned} f_{Y_1}(x) =& \sum_{j=1}^{\rho(\mathcal{A})}\sum_{h=1}^{\theta_j(\mathcal{A})}\chi_{j,h}(\mathcal{A})\frac{2\mu_j^{-h}x^{(N_{\mathrm{P}}+h)/2-1}}{(h-1)!(N_{\mathrm{P}}-1)!} \\ &\times\frac{\left(\frac{\mu_j}{\beta_{\mathrm{P}}}\right)^{-(N_{\mathrm{P}}-h)/2}}{(\beta_{\mathrm{P}})^{N_{\mathrm{P}}}}K_{N_{\mathrm{P}}-h}\left(2\sqrt{\frac{x}{\beta_{\mathrm{P}}\mu_j}}\right) \end{aligned} \tag{7}$$

where $\mathcal{A}=\mathrm{diag}\{\alpha_1^P,\ldots,\alpha_K^{\mathrm{P}}\}$ is a $K\times K$ diagonal matrix, $\rho(\mathcal{A})$ is the number of distinct diagonal elements of $\mathcal{A}$, $\mu_1,\ldots,\mu_{\rho(A)}$ are the distinct diagonal elements in decreasing order, $\theta_j(\mathcal{A})$ is the multiplicity of μ_j, $\chi_{j,h}(\mathcal{A})$ is the (j,h)th characteristic coefficient of $\mathcal{A}$, which is defined in [14, Definition 4], and $K_{\nu}(\cdot)$ is the modified Bessel function of the second kind [13, (8.432.6)].

Proof: Please refer to Appendix A. ■

With the help of Proposition 1, the exact average achievable rate can be readily obtained as $\bar{R}=\mathbb{E}\{\log_2(1+\gamma_1)\}$.

Corollary 1: Using Jensen's inequality, we derive a tight lower bound on the average achievable rate as

$$\bar{R}_L = \log_2(1+\mathrm{e}^{\Delta}) \tag{8}$$

where $\Delta=\mathbb{E}\{\ln\gamma_1\}=\mathbb{E}\{\ln(X_1/(\varepsilon P_{\mathrm{P}}Y_1+1))\}$, and the closed-form expression for Δ is derived as (9), shown at the bottom of the page. In (9), $\psi(\cdot)$ is the digamma function [24], $\mathrm{Ei}(\cdot)$ is

$$\begin{aligned} \Delta =& \psi(N_{\mathrm{S}}) + \ln I_{\mathrm{P}}\beta_{\mathrm{S}} - F_{Z_1}\left(\frac{I_{\mathrm{P}}}{P_{\mathrm{S}}}\right)\ln\frac{I_{\mathrm{P}}}{P_{\mathrm{S}}} + \sum_{k=1}^{K}\frac{(-1)^{k+1}}{k!}\underbrace{\sum_{n_1=1}^{K}\cdots\sum_{n_k=1}^{K}}_{|n_1\bigcup\cdots\bigcup n_k|=k}\left[\mathrm{Ei}\left(-\frac{\alpha^{\mathrm{S}}I_{\mathrm{P}}}{P_{\mathrm{S}}}\right) - e^{-\alpha^{\mathrm{S}}I_{\mathrm{P}}/P_{\mathrm{S}}}\ln\frac{I_{\mathrm{P}}}{P_{\mathrm{S}}}\right] \\ &- \sum_{j=1}^{\rho(A)}\sum_{h=1}^{\theta_j(A)}\chi_{j,h}(A)\frac{\mu_j^{-h}\left(\frac{\mu_j}{\beta_{\mathrm{P}}}\right)^{-(N_{\mathrm{P}}-h)/2}}{(h-1)!(N_{\mathrm{P}}-1)!(\beta_{\mathrm{P}})^{N_{\mathrm{P}}}}(\varepsilon P_{\mathrm{P}})^{-(N_{\mathrm{P}}+h)/2}G_{2,4}^{4,1}\left[(\varepsilon P_{\mathrm{P}}\beta_{\mathrm{P}}\mu_j)^{-1}\middle|_{-\frac{\nu_{h,1}}{2},\frac{\nu_{h,1}}{2},-1-\nu_{h,2},-1-\nu_{h,2}}^{-1-\nu_{h,2},-\nu_{h,2}}\right] \end{aligned} \tag{9}$$

the exponential integral function [13, (8.211.1)], $\nu_{h,1} = N_{\mathrm{P}} - h$, $\nu_{h,2} = (N_{\mathrm{P}} + h)/2 - 1$, and $G_{p,q}^{m,n}\left[x \middle| \begin{matrix} a_1, \ldots, a_p \\ b_1, \ldots, b_q \end{matrix}\right]$ denotes the Meijer G function [13, (9.301)].

Proof: The proof for (9) is provided in Appendix B. ■

For large N_{S}, $\psi(N_{\mathrm{S}}) \approx \ln N_{\mathrm{S}}$ [15]; thus, we get a tight approximation for the average achievable rate, which is given by

$$\begin{aligned} \bar{R}_L^1 &\approx \log_2(1 + N_{\mathrm{S}} \mathrm{e}^{\tilde{\Delta}}) \\ &\approx \log_2 N_{\mathrm{S}} + \tilde{\Delta} \log_2 e \end{aligned} \tag{10}$$

where $\tilde{\Delta} = \Delta - \psi(N_{\mathrm{S}})$. From (10), we find that the average achievable rate scales as $\log_2 N_{\mathrm{S}}$. Accordingly, the performance difference for different numbers of antennas at the SBS can be easily evaluated using (10).

IV. Massive MIMO Analysis

Here, we examine the asymptotic performance of the system where the PBS and the SBS are equipped with massive antenna arrays. Some interesting insights will be presented. For simplicity, we consider the case where the large-scale fading effect is neglected, i.e., $\alpha_k^{\mathrm{S}} = \alpha_k^{\mathrm{P}} = \beta_{\mathrm{S}} = \beta_{\mathrm{P}} = 1$, $\forall\, k$.[1] Under this assumption and from Proposition 1, the receive SINR at the SU is rewritten as

$$\gamma_1 \overset{d}{\sim} \frac{\min\left\{\frac{I_{\mathrm{P}}}{Z_1}, P_{\mathrm{S}}\right\} Z_2}{\frac{1}{KN_{\mathrm{P}}} P_{\mathrm{P}} Y_1 + 1}. \tag{11}$$

A. Effects of Massive MIMO at Primary Systems on Secondary Network

In this part, we analyze the effects of using massive antenna arrays at the primary network on the secondary network.

1) K and N_S Are Fixed and $N_P \to \infty$: Intuitively, with a massive array, the PBS can focus its emitted energy into the spatial directions where the PUs are located. At the same time, the PBS can purposefully avoid transmitting into directions where the SU is located, and hence, the interference from the PBS is bounded as $N_{\mathrm{P}} \to \infty$. More precisely, by using the law of large numbers, we have

$$\frac{1}{KN_{\mathrm{P}}} P_{\mathrm{P}} Y_1 = \frac{P_{\mathrm{P}}}{K} \frac{\|\mathbf{h}_{\mathrm{P}}\|^2}{N_{\mathrm{P}}} \sum_{k=1}^{K} |\Upsilon_k|^2 \overset{d}{\to} \frac{P_{\mathrm{P}}}{K} \sum_{k=1}^{K} |\Upsilon_k|^2. \tag{12}$$

As a result, the receive SINR at the SU converges to a nonzero value when the number of PBS antennas goes to infinity, i.e.,

$$\gamma_1 \overset{d}{\to} \frac{\min\left\{\frac{I_{\mathrm{P}}}{Z_1}, P_{\mathrm{S}}\right\} Z_2}{\frac{P_{\mathrm{P}}}{K} \sum_{k=1}^{K} |\Upsilon_k|^2 + 1}. \tag{13}$$

[1]Same insights shown here can be obtained for the case where the large-scale fading is taken into account.

In this case, a tight lower bound on the average achievable rate is $\bar{R}_L \to \log_2(1 + \mathrm{e}^{\Delta_1})$, where

$$\begin{aligned} \Delta_1 = {} & \psi(N_{\mathrm{S}}) + \ln P_{\mathrm{S}} + \sum_{k=1}^{K} \binom{K}{k} (-1)^{k+1} \mathrm{Ei}\left(-\frac{kI_{\mathrm{P}}}{P_{\mathrm{S}}}\right) \\ & - \sum_{j=0}^{K-1} \frac{(-1)^{K-j-2}}{(K-1-j)!} \left(\frac{K}{P_{\mathrm{P}}}\right)^{K-1-j} e^{K/P_{\mathrm{P}}} \mathrm{Ei}(-K/P_{\mathrm{P}}) \\ & - \sum_{j=0}^{K-1} \frac{(-K/P_{\mathrm{P}})^{K-1-j}}{(K-1-j)!} \sum_{m=1}^{K-1-j} (m-1)! (-K/P_{\mathrm{P}})^{-m}. \end{aligned} \tag{14}$$

The proof for (14) is provided in Appendix C. From (14), we find that adding more number of PBS antennas on the SU's average achievable rate has no impact on the average achievable rate.

We next present the large-system analysis, in order to examine the effect of large number of PUs on the performance of the secondary link.

2) N_S and $\kappa_1 = N_P/K$ Are Fixed and $N_P \to \infty$: This case corresponds to the scenario where the number of PBS antennas is large but may not be much greater than the number of PUs. When K is large, the SBS transmit power has to be reduced such that the received interference at all the PUs is smaller than a given threshold I_{P}. Thus, the performance of the secondary link is significantly degraded when K is large. This observation is confirmed by the following analysis.

Since Z_1 is the maximum of K independent and identically distributed (i.i.d.) exponential RVs, the distribution of Z_1 is asymptotically normal, as $K \to \infty$. More precisely, from [16, Proposition 1], as $K \to \infty$, we have

$$Z_1 \overset{d}{\to} 1 + \ln K + \bar{Z}_1 \tag{15}$$

where $\bar{Z}_1 \sim \mathcal{N}(0, 2)$. By using (15) together with the law of large numbers, we obtain

$$\gamma_1 \to 0, \text{ as } N_{\mathrm{P}} \to \infty,\ N_{\mathrm{P}}/K = \kappa_1. \tag{16}$$

The performance of the secondary link is affected by the number of PUs via the interference and the constraint on the transmit power of the SBS. As we can see from (16), when K grows large, the power constraint effect causes a significant degradation on the secondary system performance. In this case, the SBS cannot be permitted to share the spectrum and transmit the signal to the SU.

3) $\kappa_1 = N_P/K$ and $\kappa_2 = N_S/\ln K$ Are Fixed and $N_P \to \infty$: As discussed in the previous case, when the number of PBS antennas and the number of PUs go to infinity, the receive SINR at the SU converges to zero. One possible way to overcome this problem is adding more SBS antennas. An interesting question is: *how many antennas do we need at the SBS*? From (15), we can see that Z_1 scales as $\ln K$, as K is large, whereas Z_2 in (11) scales as N_{S}. Therefore, when the number of PUs grows large, the number of SBS antennas has to grow with the same

speed as $\ln K$. As $N_{\mathrm{P}} \to \infty$ together with fixed $\kappa_1 = N_{\mathrm{P}}/K$ and $\kappa_2 = N_{\mathrm{S}}/\ln K$, we have

$$\gamma_1 \overset{d}{\sim} \frac{\min\left\{\frac{I_{\mathrm{P}}}{Z_1}, P_{\mathrm{S}}\right\} Z_2}{P_{\mathrm{P}}\frac{\|\mathbf{h}_{\mathrm{P}}\|^2}{N_{\mathrm{P}}}\frac{\sum_{k=1}^{K}|\Upsilon_k|^2}{K}+1} = \frac{\min\left\{\frac{I_{\mathrm{P}}\ln K}{Z_1}, P_{\mathrm{S}}\ln K\right\}\frac{N_{\mathrm{S}}}{\ln K}\frac{Z_2}{N_{\mathrm{S}}}}{P_{\mathrm{P}}\frac{\|\mathbf{h}_{\mathrm{P}}\|^2}{N_{\mathrm{P}}}\frac{\sum_{k=1}^{K}|\Upsilon_k|^2}{K}+1}$$
$$\overset{d}{\to} \frac{\min\left\{\frac{I_{\mathrm{P}}\ln K}{1+\ln K+Z_1}, P_{\mathrm{S}}\ln K\right\}\frac{N_{\mathrm{S}}}{\ln K}}{P_{\mathrm{P}}+1} \approx \frac{I_{\mathrm{P}}\kappa_2}{P_{\mathrm{P}}+1} \tag{17}$$

where the convergence follows from (15) together with the law of large numbers. We can see that, by using a massive array at the SBS ($N_{\mathrm{S}} \propto \ln K$), the receive SINR at the SU converges to a nonzero value. Furthermore, by increasing κ_2 (or increasing N_{S}), we can achieve an arbitrary quality-of-service (QoS) for the secondary link. In this case, the average achievable rate is $\bar{R} = \log_2(1 + (I_{\mathrm{P}}k_2/(P_{\mathrm{P}}+1)))$.

B. Power Efficiency

Here, we examine the potential of massive MIMO to reduce the transmit power. By using massive antenna arrays at the PBS, we can reduce the transmit power P_{P} proportionally to $1/N_{\mathrm{P}}$, while maintaining a desired QoS for all the PUs [17]. Using a very low transmit power at the PBS is an interesting operating point of the massive primary systems. Here, we consider the potential for power savings in the secondary network where the SBS operates in the very low transmit power regimes.

Define $P_{\mathrm{P}} \triangleq E_{\mathrm{P}}/N_{\mathrm{P}}$ and $P_{\mathrm{S}} \triangleq E_{\mathrm{S}}/N_{\mathrm{S}}$ and assume that E_{P} and E_{S} are fixed regardless of N_{P} and N_{S}. Again, by using (11) and the law of large numbers, as N_{P} and N_{S} go to infinity, we obtain

$$\gamma_1 \to E_{\mathrm{S}}. \tag{18}$$

This implies that, by using massive antenna arrays at the PBS and the SBS, we can cut the transmit power of the PBS and the SBS proportionally to $1/N_{\mathrm{P}}$ and $1/N_{\mathrm{S}}$,[2] respectively, while maintaining a given QoS. For this case, the secondary network's performance is equivalent to a single-input–single-output AWGN channel with no interference and transmit power E_{S}.

C. Imperfect CSI Knowledge

In realistic scenarios, the imperfect knowledge of the interfering channel from the SBS to the PUs poses challenges to the underlay cognitive network. The interference impinged on the PU may exceed the maximal peak interference level I_{P} during the SBS transmissions. Different from [10], where the PU and the SU are single-antenna nodes, we extend this line of work to a network consisting of multiple PUs and multiantenna PBS and SBS. Due to the independence of the channel vector from the PBS to the SU with the PBS's precoding matrix, the impact of the primary network transmission on the SU is not changeable regardless of perfect or imperfect CSI at the PBS. For simplicity, we assume that perfect CSI is available at the PBS. We show that the accuracy of CSI of the channel between the SBS and the PUs, as well as the channel between the SBS and the SU, can be relaxed as N_{S} grows large. Here, we will show that using massive MIMO can alleviate the adverse effect of imperfect CSI knowledge.

Imperfect CSI of the channel between the SBS and the kth PU can be modeled as [19]

$$\mathbf{g}_k = \delta_k^{\mathrm{S}}\hat{\boldsymbol{g}}_k + \left(\sqrt{1-(\delta_k^{\mathrm{S}})^2}\right)\mathbf{e}_k \tag{19}$$

where $\mathbf{g}_k \sim \mathcal{CN}_{1\times N_{\mathrm{S}}}(\mathbf{0}_{1\times N_{\mathrm{S}}}, \mathbf{I}_{N_{\mathrm{S}}})$ is the true channel vector, $\hat{\boldsymbol{g}}_k \sim \mathcal{CN}_{1\times N_{\mathrm{S}}}(\mathbf{0}_{1\times N_{\mathrm{S}}}, \mathbf{I}_{N_{\mathrm{S}}})$ is the channel estimate available at the SBS, and $\mathbf{e}_k \sim \mathcal{CN}_{1\times N_{\mathrm{S}}}(\mathbf{0}_{1\times N_{\mathrm{S}}}, \mathbf{I}_{N_{\mathrm{S}}})$ is an i.i.d. Gaussian noise term. The correlation coefficient δ_k^{S} measures the accuracy of the channel estimation, i.e., $\delta_k^{\mathrm{S}} = 1$ corresponds to perfect CSI, $\delta_k^{\mathrm{S}} = 0$ corresponds to no CSI knowledge, and $\delta_k^{\mathrm{S}} \in (0,1)$ represents partial CSI.[3] Likewise, imperfect CSI about the channel between the SBS and the SU is

$$\mathbf{g}_{\mathrm{S}} = \sigma\hat{\boldsymbol{g}}_{\mathrm{S}} + (\sqrt{1-\sigma^2})\mathbf{e}_{\mathrm{S}} \tag{20}$$

where $\mathbf{g}_{\mathrm{S}} \sim \mathcal{CN}_{1\times N_{\mathrm{S}}}(\mathbf{0}_{1\times N_{\mathrm{S}}}, \mathbf{I}_{N_{\mathrm{S}}})$ is the true channel vector, $\hat{\boldsymbol{g}}_{\mathrm{S}} \sim \mathcal{CN}_{1\times N_{\mathrm{S}}}(\mathbf{0}_{1\times N_{\mathrm{S}}}, \mathbf{I}_{N_{\mathrm{S}}})$ is the channel estimate, and $\mathbf{e}_{\mathrm{S}} \sim \mathcal{CN}_{1\times N_{\mathrm{S}}}(\mathbf{0}_{1\times N_{\mathrm{S}}}, \mathbf{I}_{N_{\mathrm{S}}})$ is an i.i.d. Gaussian noise term. The parameter σ $(0 \le \sigma \le 1)$ is the correlation coefficient. Similar to [10] and [19], we assume that the correlation coefficient is a constant value.

We still consider the MRT beamforming at the SBS.[4] The interference power at the kth PU is written as

$$P_{\mathrm{t}}\lambda_k^{\mathrm{S}} = \min\left\{\frac{I_{\mathrm{P}}}{\hat{Z}_1}, P_{\mathrm{S}}\right\}\lambda_k^{\mathrm{S}} \tag{21}$$

where $\lambda_k^{\mathrm{S}} = |\mathbf{g}_k(\hat{\boldsymbol{g}}_{\mathrm{S}}^{\dagger}/\|\hat{\boldsymbol{g}}_{\mathrm{S}}^{\dagger}\|)|^2$, and $\hat{Z}_1 = \max_k\{|\hat{\boldsymbol{g}}_k(\hat{\boldsymbol{g}}_{\mathrm{S}}^{\dagger}/\|\hat{\boldsymbol{g}}_{\mathrm{S}}^{\dagger}\|)|^2\}$. The receive SINR at the SU becomes

$$\gamma_1 = \frac{\min\left\{\frac{I_{\mathrm{P}}}{\hat{Z}_1}, P_{\mathrm{S}}\right\}\sigma^2\left\|\hat{\boldsymbol{g}}_{\mathrm{S}}^{\dagger}\right\|^2}{\frac{1}{KN_{\mathrm{P}}}P_{\mathrm{P}}Y_1 + (1-\sigma^2)\min\left\{\frac{I_{\mathrm{P}}}{\hat{Z}_1}, P_{\mathrm{S}}\right\}\frac{\hat{\boldsymbol{g}}_{\mathrm{S}}\mathbb{E}\{\mathbf{e}_{\mathrm{S}}^{\dagger}\mathbf{e}_{\mathrm{S}}\}\hat{\boldsymbol{g}}_{\mathrm{S}}^{\dagger}}{\|\hat{\boldsymbol{g}}_{\mathrm{S}}^{\dagger}\|^2}+1}$$
$$= \frac{\sigma^2\min\left\{\frac{I_{\mathrm{P}}}{\hat{Z}_1}, P_{\mathrm{S}}\right\}\left\|\hat{\boldsymbol{g}}_{\mathrm{S}}^{\dagger}\right\|^2}{\frac{1}{KN_{\mathrm{P}}}P_{\mathrm{P}}Y_1 + (1-\sigma^2)\min\left\{\frac{I_{\mathrm{P}}}{\hat{Z}_1}, P_{\mathrm{S}}\right\}+1}. \tag{22}$$

We next show the benefits of massive antenna arrays at the secondary network with imperfect CSI knowledge. To this end, two important cases are examined as follows.

1) $N_S \to \infty$ and K and N_P Are Fixed: This case corresponds to the scenario where massive antenna arrays are only used at the secondary network.

We first examine the interference leakage probability. An interference leakage is declared when the interference power at the kth PU is larger than the peak allowable interference

[2]Here, we have ignored the increase of the circuit power consumption due to more antennas, as in [17]. The investigation of circuit power consumption with massive MIMO is found in [18].

[3]As mentioned in [19], the correlation coefficient can be extended to an arbitrary function of the system parameters.

[4]The linear transmission scheme can achieve the optimality with large arrays [20], [21].

power I_{P}. Based on (21), the interference leakage probability is upper bounded as

$$\Pr\left(P_{\mathrm{t}}\lambda_k^{\mathrm{S}} > I_{\mathrm{p}}\right) = \Pr\left(\min\left\{\frac{I_{\mathrm{P}}}{\hat{Z}_1}, P_{\mathrm{S}}\right\}\lambda_k^{\mathrm{S}} > I_{\mathrm{p}}\right) < \Pr\left(P_{\mathrm{S}}\lambda_k^{\mathrm{S}} > I_{\mathrm{p}}\right) = e^{-\frac{I_{\mathrm{P}}}{P_{\mathrm{S}}}}. \quad (23)$$

Here, λ_k^{S} follows the exponential distribution with unit mean, as suggested in Appendix A. From (23), we find that reducing the SBS's transmit power can decrease the interference leakage probability. For low transmit power of $P_{\mathrm{S}} \to 0$, $\Pr(P_{\mathrm{t}}\lambda_k^{\mathrm{S}} > I_{\mathrm{p}}) \to 0$, which implies that an arbitrary small value of the interference leakage probability can be achieved.

In the secondary network, the receive SINR at the SU given in (22) becomes

$$\gamma_1 \xrightarrow{d} \frac{\sigma^2 \min\left\{\frac{I_{\mathrm{P}}}{\hat{Z}_1}, P_{\mathrm{S}}\right\} N_{\mathrm{S}}}{\frac{1}{KN_{\mathrm{P}}}P_{\mathrm{P}}Y_1 + (1-\sigma^2)\min\left\{\frac{I_{\mathrm{P}}}{\hat{Z}_1}, P_{\mathrm{S}}\right\} + 1}. \quad (24)$$

Based on (24), the average achievable rate is $\bar{R}_L \to \log_2(1 + \mathrm{e}^{\Delta_2})$, where Δ_2 is provided in Appendix D.

For low transmit power of $P_{\mathrm{S}} \to 0$, the receive SINR at the SU in (24) reduces to

$$\gamma_1 \xrightarrow{d} \frac{\sigma^2 P_{\mathrm{S}} N_{\mathrm{S}}}{\frac{1}{KN_{\mathrm{P}}}P_{\mathrm{P}}Y_1 + (1-\sigma^2)P_{\mathrm{S}} + 1}. \quad (25)$$

In (25), the interference term $(1-\sigma^2)P_{\mathrm{S}}$ resulting from channel estimation error can be arbitrarily small, as $P_{\mathrm{S}} \to 0$. Based on (25), the average achievable rate reduces to

$$\bar{R}_L \to \log_2(1 + \mathrm{e}^{\Delta_3}) \quad (26)$$

where $\Delta_3 = \ln N_{\mathrm{S}} + \ln[\sigma^2 P_{\mathrm{S}}/(1+(1-\sigma^2)P_{\mathrm{S}})] - ((\varpi_1)^{-(N_{\mathrm{P}}+K)/2}/(N_{\mathrm{P}}-1)!(K-1)!)G_{2,4}^{4,1}[(\varpi_1)^{-1}|_{-(\varpi_2/2),\varpi_2/2,-1-\varpi_3,-1-\varpi_3}^{-1-\varpi_3,-\varpi_3}]$, with $\varpi_1 = (P_{\mathrm{P}}/KN_{\mathrm{P}})/(1+(1-\sigma^2)P_{\mathrm{S}})$, $\varpi_2 = N_{\mathrm{P}} - K$, and $\varpi_3 = (N_{\mathrm{P}}+K)/2 - 1$.

Remark 1: It is shown from (24) and (25) that the receive SINR at the SU is proportional to N_{S} under imperfect CSI, which, in turn, implies that we can still cut the transmit power at the SBS proportionally to $1/N_{\mathrm{S}}$, while maintaining a given QoS. In addition, reducing the SBS's transmit power can reduce the interference term $(1-\sigma^2)\min\{I_{\mathrm{P}}/\hat{Z}_1, P_{\mathrm{S}}\}$, which results from the imperfect channel estimation.

Remark 2: Based on Remark 1, (23), and (25), reducing the SBS's transmit power proportionally to $1/N_{\mathrm{S}}$ reduces the interference leakage probability. Therefore, the detrimental effect of imperfect CSI in cognitive radio networks can be significantly mitigated when the SBS is equipped with large antenna arrays.

2) $\kappa_1 = N_{\mathrm{P}}/K$ and $\kappa_2 = N_{\mathrm{S}}/\ln K$ Are Fixed and $N_{\mathrm{P}} \to \infty$: The significance of this case has been mentioned in Sections IV-A2 and IV-A3. In this case, we have $\min\{I_{\mathrm{P}}/Z_1, P_{\mathrm{S}}\} \to (I_{\mathrm{P}}/\ln K)$ (as illustrated in Section IV-A3); hence, $P_{\mathrm{t}}\lambda_k^{\mathrm{S}} \to (I_{\mathrm{P}}\lambda_k^{\mathrm{S}}/\ln K)$. The interference leakage probability becomes

$$\Pr\left(P_{\mathrm{t}}\lambda_k^{\mathrm{S}} > I_{\mathrm{p}}\right) \to \Pr\left(\frac{I_{\mathrm{P}}\lambda_k^{\mathrm{S}}}{\ln K} > I_{\mathrm{p}}\right) = e^{-\ln K}. \quad (27)$$

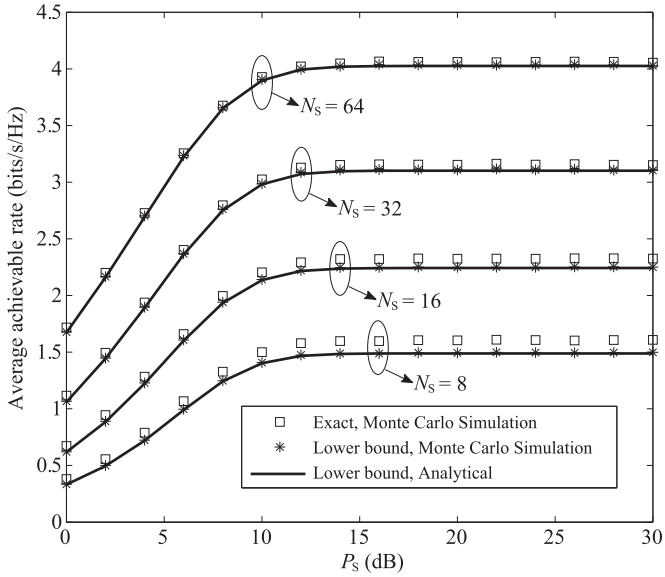

Fig. 2. Average achievable rate versus P_{S} for $N_{\mathrm{P}} = 16$, $K = 5$, $I_{\mathrm{P}} = 10$ dB, $P_{\mathrm{P}} = 15$ dB.

Based on (27), we find that an arbitrary small value of interference leakage probability can be achieved, when the number of PBS antennas goes to infinity.

With the assistance of (17) and (24), the receive SINR at the SU becomes

$$\gamma_1 \xrightarrow{d} \frac{\sigma^2 \frac{I_{\mathrm{P}}}{\ln K} N_{\mathrm{S}}}{P_{\mathrm{P}} + (1-\sigma^2)\frac{I_{\mathrm{P}}}{\ln K} + 1} \approx \frac{\sigma^2 I_{\mathrm{P}} N_{\mathrm{S}}}{(P_{\mathrm{P}}+1)\ln K}. \quad (28)$$

It is indicated from (28) that the detrimental effect of imperfect CSI at the SBS vanishes when the number of SBS antennas grows large. In this case, the average achievable rate is $\bar{R} \to \log_2(1 + (\sigma^2 I_{\mathrm{P}} N_{\mathrm{S}}/(P_{\mathrm{P}}+1)\ln K)$.

V. Numerical Results

Here, numerical results are presented to verify our analysis. We first consider a practical scenario that different links may have different large-scale fading coefficients. This setting enables us to validate the expression for the average achievable rate. We also show the accuracy of our massive MIMO analysis. We focus on the average achievable rate in the secondary network.

Fig. 2 plots the average achievable rate versus the SBS's maximum transmit power P_{S} for different numbers of antennas at the SBS. The large-scale fading coefficients are set as $\beta_{\mathrm{S}} = \beta_{\mathrm{P}} = 1$, $[\alpha_1^{\mathrm{P}}, \alpha_2^{\mathrm{P}}, \alpha_3^{\mathrm{P}}, \alpha_4^{\mathrm{P}}, \alpha_5^{\mathrm{P}}] = [0.5, 0.7, 1, 0.65, 0.6]$, and $[\alpha_1^{\mathrm{S}}, \alpha_2^{\mathrm{S}}, \alpha_3^{\mathrm{S}}, \alpha_4^{\mathrm{S}}, \alpha_5^{\mathrm{S}}] = [0.8, 1, 0.6, 0.7, 0.4]$. The analytical curves for the lower bound of the average achievable rate are obtained from (8), which are tightly matched to the exact Monte Carlo simulations. As suggested, the average achievable rate increases with increasing number of antennas at the SBS. Due to the interference constraint, there exist rate ceilings at high signal-to-noise ratio (SNR).

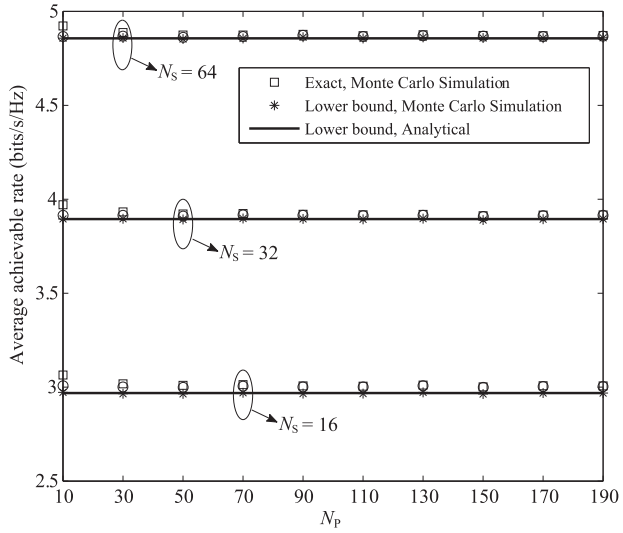

Fig. 3. Average achievable rate versus N_{P} for $K = 6$, $I_{\mathrm{P}} = 10$ dB, $P_{\mathrm{P}} = 10$ dB, $P_{\mathrm{S}} = 10$ dB.

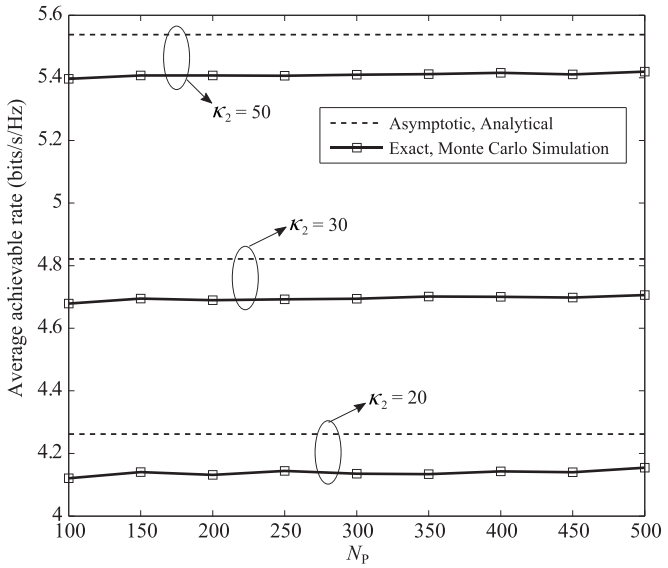

Fig. 4. Average achievable rate versus N_{P} for $\kappa_1 = 5$, $I_{\mathrm{P}} = 10$ dB, $P_{\mathrm{P}} = 10$ dB, $P_{\mathrm{S}} = 15$ dB.

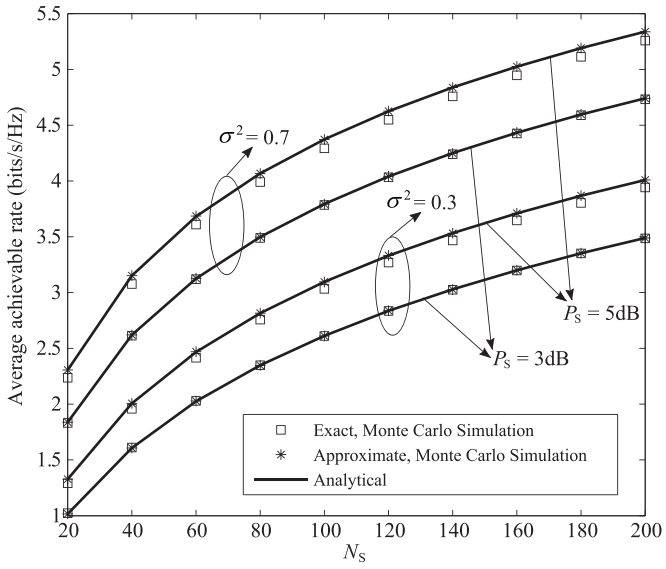

Fig. 5. Average achievable rate versus N_{S} for $K = 6$, $N_{\mathrm{P}} = 64$, $I_{\mathrm{P}} = 10$ dB, $P_{\mathrm{P}} = 10$ dB.

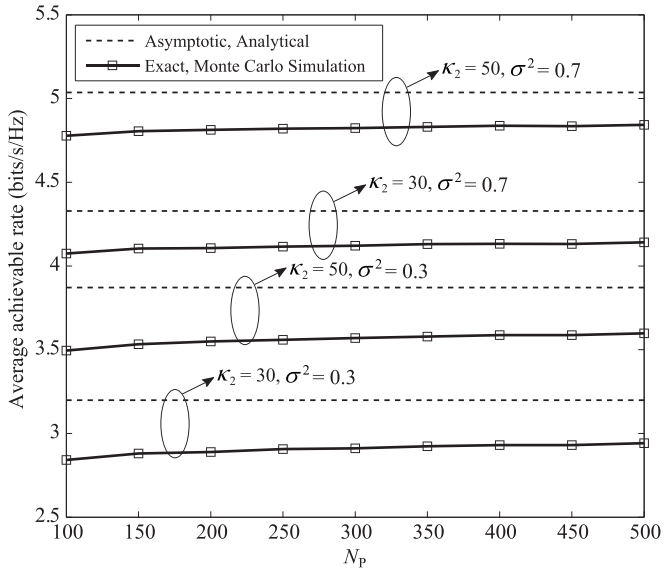

Fig. 6. Average achievable rate versus N_{P} for $\kappa_1 = 5$, $I_{\mathrm{P}} = 10$ dB, $P_{\mathrm{P}} = 10$ dB, $P_{\mathrm{S}} = 10$ dB.

Fig. 3 plots the average achievable rate for the case that K and N_{S} are fixed and $N_{\mathrm{P}} \to \infty$ in Section IV-A1. The analytical and Monte Carlo simulated curves for the lower bound of average achievable rate are obtained based on (13). Our asymptotic analysis for large N_{P} is in a strong agreement with the exact Monte Carlo simulation. As mentioned in Section IV-A1, increasing number of antennas at the PBS has negligible effect on the average achievable rate. The average achievable rate increases with increasing number of SBS antennas.

Fig. 4 plots the average achievable rate for the case that $\kappa_1 = N_{\mathrm{P}}/K$ and $\kappa_2 = N_{\mathrm{S}}/\ln K$ are fixed and $N_{\mathrm{P}} \to \infty$ in Section IV-A3. The asymptotic analytical curves are obtained based on (17). Our asymptotic analysis can well predict the performance behavior. As suggested in Section IV-A3, increasing the number of PBS antennas has negligible effect on the average achievable rate. The average achievable rate is improved by increasing κ_2 (increasing N_{S}).

Fig. 5 plots the average achievable rate with imperfect CSI for the case that $N_{\mathrm{S}} \to \infty$ and K and N_{P} are fixed in Section IV-C1. The channel estimation accuracy coefficients are assumed to be $\delta_1^{\mathrm{S}} = \cdots = \delta_K^{\mathrm{S}} = \sigma$. The analytical curves for approximate average achievable rate are obtained from (26). Our approximate analysis has a tight match with the exact Monte Carlo simulations, particularly in the low-SNR regime. As predicted, the accuracy of channel estimation has a big effect on the average achievable rate. The average achievable rate improves with increasing N_{S}. Due to the large array gain, the transmit power can be saved, and the channel estimation accuracy can be alleviated for a given average achievable rate value.

Fig. 6 plots the average achievable rate with imperfect CSI for the case that $\kappa_1 = N_{\mathrm{P}}/K$ and $\kappa_2 = N_{\mathrm{S}}/\ln K$ are fixed and $N_{\mathrm{P}} \to \infty$ in Section IV-C2. The channel estimation accuracy coefficients are assumed to be $\delta_1^{\mathrm{S}} = \cdots = \delta_K^{\mathrm{S}} = \sigma$. The asymptotic analytical curves are obtained based on (28). Our asymptotic analysis can well predict the average achievable rate. It is observed that the exact Monte Carlo simulations slowly converge to the asymptotic results with increasing N_{P}. The average achievable rate decreases with lowering the channel estimation accuracy and improves with increasing κ_2 (increasing N_{S}).

VI. Conclusion

In this paper, we have considered the application of massive MIMO in spectrum sharing networks. We first derived a tight lower bound of the average achievable rate, which can be used to measure the performance for any finite numbers of antennas. We then presented the asymptotic analysis for massive antenna arrays at the PBS and the SBS. In particular, we analyzed the impact of large number of PUs on the secondary networks. The impact of imperfect CSI in the secondary network was also examined. Based on our analysis, we clearly established the importance of using massive MIMO in the future spectrum sharing networks for 5G. For future work, the adoption of the peak interference level in massive MIMO spectrum sharing networks would be of interest.

Appendix A
Proof of Proposition 1

We first derive the PDF of X_1. Conditioned on $\mathbf{g}_{\mathrm{S}}$, $\mathbf{g}_k(\mathbf{g}_{\mathrm{S}}^\dagger/\|\mathbf{g}_{\mathrm{S}}^\dagger\|)$ is a complex Gaussian RV with zero mean and variance α_k^{S}. Since the PDF of a complex Gaussian RV is fully described via its first and second moments, $\mathbf{g}_k(\mathbf{g}_{\mathrm{S}}^\dagger/\|\mathbf{g}_{\mathrm{S}}^\dagger\|)$ is a complex Gaussian RV, which is independent of $\mathbf{g}_{\mathrm{S}}$. As such, the cumulative density function (CDF) of Z_1 is

$$\begin{aligned} F_{Z_1}(x) &= \Pr\left(\max_k \left\{\left|\mathbf{g}_k \frac{\mathbf{g}_{\mathrm{S}}^\dagger}{\left\|\mathbf{g}_{\mathrm{S}}^\dagger\right\|}\right|^2\right\} < x\right) \\ &= \prod_{k=1}^{K}\left(1 - e^{-x/\alpha_k^{\mathrm{S}}}\right) \\ &= 1 + \sum_{k=1}^{K}\frac{(-1)^k}{k!}\underbrace{\sum_{n_1=1}^{K}\cdots\sum_{n_k=1}^{K}}_{|n_1\bigcup\cdots\bigcup n_k|=k} e^{-\alpha^{\mathrm{S}}x}. \end{aligned} \tag{29}$$

Taking the derivative of (29), we obtain the PDF of Z_1 as

$$f_{Z_1}(x) = \sum_{k=1}^{K}\frac{(-1)^{k+1}}{k!}\underbrace{\sum_{n_1=1}^{K}\cdots\sum_{n_k=1}^{K}}_{|n_1\bigcup\cdots\bigcup n_k|=k}\alpha^{\mathrm{S}}e^{-\alpha^{\mathrm{S}}x}. \tag{30}$$

In addition, the PDF of Z_2 is given by [22]

$$f_{Z_2}(x) = \frac{x^{N_{\mathrm{S}}-1}e^{-x/\beta_{\mathrm{S}}}}{(N_{\mathrm{S}}-1)!(\beta_{\mathrm{S}})^{N_{\mathrm{S}}}}. \tag{31}$$

The CDF of X_1 is expressed as

$$\begin{aligned} F_{X_1}(x) &= \Pr\left\{\min\left(\frac{I_{\mathrm{P}}}{Z_1}, P_{\mathrm{S}}\right) Z_2 < x\right\} \\ &= \underbrace{\Pr\left\{Z_2 < \frac{x}{P_{\mathrm{S}}}, Z_1 < \frac{I_{\mathrm{P}}}{P_{\mathrm{S}}}\right\}}_{J_1} \\ &\quad + \underbrace{\Pr\left\{\frac{Z_2}{Z_1} < \frac{x}{I_{\mathrm{P}}}, Z_1 \geq \frac{I_{\mathrm{P}}}{P_{\mathrm{S}}}\right\}}_{J_2}. \end{aligned} \tag{32}$$

Noting that Z_1 and Z_2 are independent, it is easy to see that

$$J_1 = F_{Z_2}\left(\frac{x}{P_{\mathrm{S}}}\right)F_{Z_1}\left(\frac{I_{\mathrm{P}}}{P_{\mathrm{S}}}\right) \tag{33}$$

where $F_{Z_2}(x)$ is the CDF of Z_2. In addition, J_2 is derived as

$$J_2 = \int_{\frac{I_{\mathrm{P}}}{P_{\mathrm{S}}}}^{\infty} F_{Z_2}\left(\frac{xt}{I_{\mathrm{P}}}\right) f_{Z_1}(t)dt. \tag{34}$$

Based on (32), the PDF of X_1 is

$$f_{X_1}(x) = \frac{\partial J_1}{\partial x} + \frac{\partial J_2}{\partial x}. \tag{35}$$

From (33), we obtain

$$\frac{\partial J_1}{\partial x} = \frac{1}{P_{\mathrm{S}}}f_{Z_2}\left(\frac{x}{P_{\mathrm{S}}}\right)F_{Z_1}\left(\frac{I_{\mathrm{P}}}{P_{\mathrm{S}}}\right). \tag{36}$$

Substituting (31) into (36), we obtain

$$\frac{\partial J_1}{\partial x} = F_{Z_1}\left(\frac{I_{\mathrm{P}}}{P_{\mathrm{S}}}\right)\frac{x^{N_{\mathrm{S}}-1}e^{-\frac{x}{P_{\mathrm{S}}\beta_{\mathrm{S}}}}}{(N_{\mathrm{S}}-1)!(P_{\mathrm{S}}\beta_{\mathrm{S}})^{N_{\mathrm{S}}}}. \tag{37}$$

From (34), we observe that

$$\frac{\partial J_2}{\partial x} = \int_{\frac{I_{\mathrm{P}}}{P_{\mathrm{S}}}}^{\infty}\frac{t}{I_{\mathrm{P}}}f_{Z_2}\left(\frac{xt}{I_{\mathrm{P}}}\right)f_{Z_1}(t)dt. \tag{38}$$

Plugging (30) and (31) into (38), after some algebraic manipulations, we obtain

$$\begin{aligned} \frac{\partial J_2}{\partial x} &= \sum_{k=1}^{K}\frac{(-1)^{k+1}}{k!}\underbrace{\sum_{n_1=1}^{K}\cdots\sum_{n_k=1}^{K}}_{|n_1\bigcup\cdots\bigcup n_k|=k}\alpha^{\mathrm{S}}\frac{x^{N_{\mathrm{S}}-1}}{(N_{\mathrm{S}}-1)!(I_{\mathrm{P}}\beta_{\mathrm{S}})^{N_{\mathrm{S}}}} \\ &\quad\times\int_{\frac{I_{\mathrm{P}}}{P_{\mathrm{S}}}}^{\infty} t^{N_{\mathrm{S}}}e^{-\left(\frac{x}{I_{\mathrm{P}}\beta_{\mathrm{S}}}+\alpha^{\mathrm{S}}\right)t}dt \\ &= \sum_{k=1}^{K}\frac{(-1)^{k+1}}{k!}\underbrace{\sum_{n_1=1}^{K}\cdots\sum_{n_k=1}^{K}}_{|n_1\bigcup\cdots\bigcup n_k|=k}\alpha^{\mathrm{S}}\frac{x^{N_{\mathrm{S}}-1}\left(\frac{x}{I_{\mathrm{P}}\beta_{\mathrm{S}}}+\alpha^{\mathrm{S}}\right)^{-(N_{\mathrm{S}}+1)}}{(N_{\mathrm{S}}-1)!(I_{\mathrm{P}}\beta_{\mathrm{S}})^{N_{\mathrm{S}}}} \\ &\quad\times\Gamma\left(N_{\mathrm{S}}+1, \frac{x}{P_{\mathrm{S}}\beta_{\mathrm{S}}}+\frac{I_{\mathrm{P}}\alpha^{\mathrm{S}}}{P_{\mathrm{S}}}\right). \end{aligned} \tag{39}$$

Based on (35), (37), and (39), we obtain the desired expression for the PDF of X_1 as (6).

We next derive the PDF of Y_1. Y_1 can be rewritten as $Y_1 = \xi_1\xi_2$, where $\xi_1 = \|\mathbf{h}_{\mathrm{P}}\|^2$, and $\xi_2 = \sum_{k=1}^{K}|\Upsilon_k|^2$, with $\Upsilon_k = (\mathbf{h}_{\mathrm{P}}/\|\mathbf{h}_{\mathrm{P}}\|)\mathbf{h}_k^{\dagger}$. We see that Υ_k is a complex Gaussian RV with zero mean and variance α_k^{P}, which is independent of $\mathbf{h}_{\mathrm{P}}$. The PDF of ξ_1 is given by

$$f_{\xi_1}(x) = \frac{x^{N_{\mathrm{P}}-1}e^{-x/\beta_{\mathrm{P}}}}{(N_{\mathrm{P}}-1)!(\beta_{\mathrm{P}})^{N_{\mathrm{P}}}} \tag{40}$$

and the PDF of ξ_2 is given by [23]

$$f_{\xi_2}(x) = \sum_{j=1}^{\rho(\mathcal{A})}\sum_{h=1}^{\theta_j(\mathcal{A})}\chi_{j,h}(\mathcal{A})\frac{\mu_j^{-h}}{(h-1)!}x^{h-1}e^{-\frac{x}{\mu_j}}. \tag{41}$$

Since ξ_1 and ξ_2 are independent, the CDF of Y_1 is written as

$$\begin{aligned}F_{Y_1}(x) &= \Pr(\xi_1\xi_2 < x)\\ &= \int_0^{\infty} F_{\xi_1}\left(\frac{x}{t}\right)f_{\xi_2}(t)dt.\end{aligned} \tag{42}$$

Taking the derivative of $F_{Y_1}(x)$ in (7), we obtain the PDF of Y_1 as

$$\begin{aligned}f_{Y_1}(x) &= \int_0^{\infty}\frac{1}{t}f_{\xi_1}\left(\frac{x}{t}\right)f_{\xi_2}(t)dt\\ &= \sum_{j=1}^{\rho(A)}\sum_{h=1}^{\theta_j(A)}\chi_{j,h}(A)\frac{\mu_j^{-h}x^{N_{\mathrm{P}}-1}}{(h-1)!(N_{\mathrm{P}}-1)!(\beta_{\mathrm{P}})^{N_{\mathrm{P}}}}\\ &\quad\times\int_0^{\infty}\frac{1}{t^{N_{\mathrm{P}}-h+1}}e^{-x/t\beta_{\mathrm{P}}}e^{-\frac{t}{\mu_j}}dt.\end{aligned} \tag{43}$$

After calculating the integral, we obtain (7).

APPENDIX B
DETAILED DERIVATION OF (9)

From (8), we calculate Δ as

$$\Delta = \mathbb{E}\{\ln X_1\} - \mathbb{E}\left\{\ln(\varepsilon P_{\mathrm{P}}Y_1+1)\right\}. \tag{44}$$

In (44), $\mathbb{E}\{\ln X_1\}$ is derived as

$$\begin{aligned}\mathbb{E}\{\ln X_1\} &= \int_0^{\infty}\ln x f_{X_1}(x)dx\\ &= F_{Z_1}\left(\frac{I_{\mathrm{P}}}{P_{\mathrm{S}}}\right)\frac{1}{(N_{\mathrm{S}}-1)!(P_{\mathrm{S}}\beta_{\mathrm{S}})^{N_{\mathrm{S}}}}\underbrace{\int_0^{\infty}x^{N_{\mathrm{S}}-1}e^{-\frac{x}{P_{\mathrm{S}}\beta_{\mathrm{S}}}}\ln x dx}_{\Xi_1}\\ &\quad+\sum_{k=1}^{K}\frac{(-1)^{k+1}}{k!}\underbrace{\sum_{n_1=1}^{K}\cdots\sum_{n_k=1}^{K}}_{|n_1\bigcup\cdots\bigcup n_k|=k}\frac{\alpha^{\mathrm{S}}}{(N_{\mathrm{S}}-1)!(I_{\mathrm{P}}\beta_{\mathrm{S}})^{N_{\mathrm{S}}}}\\ &\quad\times\int_0^{\infty}x^{N_{\mathrm{S}}-1}\left(\frac{x}{I_{\mathrm{P}}\beta_{\mathrm{S}}}+\alpha^{\mathrm{S}}\right)^{-(N_{\mathrm{S}}+1)}\\ &\quad\times\underbrace{\Gamma\left(N_{\mathrm{S}}+1,\frac{x}{P_{\mathrm{S}}\beta_{\mathrm{S}}}+\frac{I_{\mathrm{P}}\alpha^{\mathrm{S}}}{P_{\mathrm{S}}}\right)\ln x dx}_{\Xi_2}.\end{aligned} \tag{45}$$

Using $\int_0^{\infty}x^{v-1}e^{-\mu x}\ln x dx = \mu^{-v}\Gamma(v)(\psi(v)-\ln\mu)$ [13, (4.352.1)], Ξ_1 is calculated as

$$\Xi_1 = (P_{\mathrm{S}}\beta_{\mathrm{S}})^{N_{\mathrm{S}}}(N_{\mathrm{S}}-1)!\left(\psi(N_{\mathrm{S}})+\ln P_{\mathrm{S}}\beta_{\mathrm{S}}\right). \tag{46}$$

Changing the order of integration and using [13, (4.352.1)], after some manipulations, Ξ_2 is evaluated as

$$\begin{aligned}\Xi_2 &= \int_0^{\infty}x^{N_{\mathrm{S}}-1}\ln x\int_{\frac{I_{\mathrm{P}}}{P_{\mathrm{S}}}}^{\infty}t^{N_{\mathrm{S}}}e^{-\left(\frac{x}{I_{\mathrm{P}}\beta_{\mathrm{S}}}+\alpha^{\mathrm{S}}\right)t}dtdx\\ &= \int_{\frac{I_{\mathrm{P}}}{P_{\mathrm{S}}}}^{\infty}t^{N_{\mathrm{S}}}e^{-\alpha^{\mathrm{S}}t}\int_0^{\infty}e^{-\frac{x}{I_{\mathrm{P}}\beta_{\mathrm{S}}}t}x^{N_{\mathrm{S}}-1}\ln x dxdt\\ &= (I_{\mathrm{P}}\beta_{\mathrm{S}})^{N_{\mathrm{S}}}\frac{(N_{\mathrm{S}}-1)!}{\alpha^{\mathrm{S}}}\Big[\left(\psi(N_{\mathrm{S}})+\ln I_{\mathrm{P}}\beta_{\mathrm{S}}\right)e^{-\alpha^{\mathrm{S}}I_{\mathrm{P}}/P_{\mathrm{S}}}\\ &\qquad-e^{-\alpha^{\mathrm{S}}I_{\mathrm{P}}/P_{\mathrm{S}}}\ln\frac{I_{\mathrm{P}}}{P_{\mathrm{S}}}+\mathrm{Ei}\left(-\frac{\alpha^{\mathrm{S}}I_{\mathrm{P}}}{P_{\mathrm{S}}}\right)\Big].\end{aligned} \tag{47}$$

Substituting (46) and (47) into (45), after some manipulations, we obtain

$$\begin{aligned}\mathbb{E}\{\ln X_1\} &= \psi(N_{\mathrm{S}})+\ln I_{\mathrm{P}}\beta_{\mathrm{S}}-F_{Z_1}\left(\frac{I_{\mathrm{P}}}{P_{\mathrm{S}}}\right)\ln\frac{I_{\mathrm{P}}}{P_{\mathrm{S}}}\\ &\quad+\sum_{k=1}^{K}\frac{(-1)^{k+1}}{k!}\underbrace{\sum_{n_1=1}^{K}\cdots\sum_{n_k=1}^{K}}_{|n_1\bigcup\cdots\bigcup n_k|=k}\\ &\quad\left[\mathrm{Ei}\left(-\frac{\alpha^{\mathrm{S}}I_{\mathrm{P}}}{P_{\mathrm{S}}}\right)-e^{-\alpha^{\mathrm{S}}I_{\mathrm{P}}/P_{\mathrm{S}}}\ln\frac{I_{\mathrm{P}}}{P_{\mathrm{S}}}\right].\end{aligned} \tag{48}$$

In addition, $\mathbb{E}\{\ln(\varepsilon P_{\mathrm{P}}Y_1+1)\}$ is derived as

$$\begin{aligned}&\mathbb{E}\left\{\ln(\varepsilon P_{\mathrm{P}}Y_1+1)\right\}\\ &= \int_0^{\infty}\ln\left(\varepsilon P_{\mathrm{P}}x+1\right)f_{Y_1}(x)dx\\ &= \sum_{j=1}^{\rho(\mathcal{A})}\sum_{h=1}^{\theta_j(\mathcal{A})}\chi_{j,h}(\mathcal{A})\frac{2\mu_j^{-h}\left(\frac{\mu_j}{\beta_{\mathrm{P}}}\right)^{-(N_{\mathrm{P}}-h)/2}}{(h-1)!(N_{\mathrm{P}}-1)!(\beta_{\mathrm{P}})^{N_{\mathrm{P}}}}\\ &\quad\times\int_0^{\infty}x^{(N_{\mathrm{P}}+h)/2-1}\ln(\varepsilon P_{\mathrm{P}}x+1)K_{N_{\mathrm{P}}-h}\left(2\sqrt{\frac{x}{\beta_{\mathrm{P}}\mu_j}}\right)dx\\ &= \sum_{j=1}^{\rho(\mathcal{A})}\sum_{h=1}^{\theta_j(\mathcal{A})}\chi_{j,h}(\mathcal{A})\frac{\mu_j^{-h}\left(\frac{\mu_j}{\beta_{\mathrm{P}}}\right)^{-(N_{\mathrm{P}}-h)/2}}{(h-1)!(N_{\mathrm{P}}-1)!(\beta_{\mathrm{P}})^{N_{\mathrm{P}}}}(\varepsilon P_{\mathrm{P}})^{-(N_{\mathrm{P}}+h)/2}\\ &\quad\times G_{2,4}^{4,1}\left[\left(\varepsilon P_{\mathrm{P}}\beta_{\mathrm{P}}\mu_j\right)^{-1}\middle|_{-\frac{\nu_{h,1}}{2},\frac{\nu_{h,1}}{2},-1-\nu_{h,2},-1-\nu_{h,2}}^{-1-\nu_{h,2},-\nu_{h,2}}\right].\end{aligned} \tag{49}$$

Substituting (48) and (49) into (44), we obtain Δ in (9).

APPENDIX C
DETAILED DERIVATION OF (14)

We derive the tight lower bound of the average achievable rate when K and N_{S} are fixed and the large-scale fading effect is neglected and $N_{\mathrm{P}} \to \infty$. Noting that $X_1 = \min\{I_{\mathrm{P}}/Z_1, P_{\mathrm{S}}\}Z_2$ and $\xi_2 = \sum_{k=1}^{K} |\Upsilon_k|^2$, the tight lower bound of the average achievable rate is given by $\bar{R}_L = \log_2(1+\mathrm{e}^{\Delta_1})$, with $\Delta_1 = \mathbb{E}\{\ln X_1\} - \mathbb{E}\{\ln((P_{\mathrm{P}}/K)\xi_2+1)\}$. In this case, $\mathbb{E}\{\ln X_1\}$ in (48) reduces to

$$\mathbb{E}\{\ln X_1\} = \psi(N_{\mathrm{S}}) + \ln P_{\mathrm{S}} + \sum_{k=1}^{K} \binom{K}{k} (-1)^{k+1} \mathrm{Ei}\left(-\frac{kI_{\mathrm{P}}}{P_{\mathrm{S}}}\right). \tag{50}$$

In addition, the PDF of ξ_2 in (41) reduces to

$$f_{\xi_2}(x) = \frac{x^{K-1}e^{-x}}{(K-1)!}. \tag{51}$$

$\mathrm{E}\{\ln((P_{\mathrm{P}}/K)\xi_2 + 1)\}$ is derived as

$$\mathrm{E}\left\{\ln\left(\frac{P_{\mathrm{P}}}{K}\xi_2 + 1\right)\right\} = \int_0^{\infty} \ln\left(\frac{P_{\mathrm{P}}}{K}x + 1\right) f_{\xi_2}(x)dx. \tag{52}$$

By employing [13, (4.337.5)], we calculate (52) as

$$\begin{aligned}
&\mathrm{E}\left\{\ln\left(\frac{P_{\mathrm{P}}}{K}\xi_2 + 1\right)\right\} \\
&\quad = \sum_{j=0}^{K-1} \frac{(-1)^{K-j-2}}{(K-1-j)!} \left(\frac{K}{P_{\mathrm{P}}}\right)^{K-1-j} e^{\frac{K}{P_{\mathrm{P}}}} \mathrm{Ei}(-K/P_{\mathrm{P}}) \\
&\qquad + \sum_{j=0}^{K-1} \frac{(-K/P_{\mathrm{P}})^{K-1-j}}{(K-1-j)!} \sum_{m=1}^{K-1-j} (m-1)!(-K/P_{\mathrm{P}})^{-m}.
\end{aligned} \tag{53}$$

Based on (50) and (53), Δ_1 is derived as (14).

APPENDIX D
DETAILED DERIVATION OF Δ_2

As suggested in Appendix C, $\Delta_2 = \mathbb{E}\{\ln X_1\} - \mathbb{E}\{\ln X_2\}$, where $X_1 = \sigma^2 \min\{I_{\mathrm{P}}/\hat{Z}_1, P_{\mathrm{S}}\}N_{\mathrm{S}}$, and $X_2 = (1/KN_{\mathrm{P}})P_{\mathrm{P}}Y_1 + (1-\sigma^2)\min\{I_{\mathrm{P}}/\hat{Z}_1, P_{\mathrm{S}}\} + 1$. We first calculate $\mathbb{E}\{\ln X_1\}$ as

$$\begin{aligned}
\mathbb{E}\{\ln X_1\} &= \ln(\sigma^2 N_{\mathrm{S}}) + \int_0^{\infty} \ln\left(\min\left\{\frac{I_{\mathrm{P}}}{x}, P_{\mathrm{S}}\right\}\right) f_{\hat{Z}_1}(x)dx \\
&= \ln(\sigma^2 N_{\mathrm{S}}) + \ln(P_{\mathrm{S}}) \int_0^{\frac{I_{\mathrm{P}}}{P_{\mathrm{S}}}} f_{\hat{Z}_1}(x)dx \\
&\quad + \int_{\frac{I_{\mathrm{P}}}{P_{\mathrm{S}}}}^{\infty} \ln\left(\frac{I_{\mathrm{P}}}{x}\right) f_{\hat{Z}_1}(x)dx \\
&= \ln(\sigma^2 N_{\mathrm{S}}) + \ln\left(\frac{P_{\mathrm{S}}}{I_{\mathrm{P}}}\right) F_{\hat{Z}_1}\left(\frac{I_{\mathrm{P}}}{P_{\mathrm{S}}}\right) + \ln(I_{\mathrm{P}}) \\
&\quad - \int_{\frac{I_{\mathrm{P}}}{P_{\mathrm{S}}}}^{\infty} \ln(x) f_{\hat{Z}_1}(x)dx.
\end{aligned} \tag{54}$$

Note that $F_{\hat{Z}_1}(x) = (1-e^{-x})^K$ and $f_{\hat{Z}_1}(x) = \sum_{k=1}^{K} \binom{K}{k} k(-1)^{k+1}e^{-kx}$. Substituting them into (54) yields

$$\begin{aligned}
\mathbb{E}\{\ln X_1\} &= \ln(\sigma^2 N_{\mathrm{S}} I_{\mathrm{P}}) + \ln\left(\frac{P_{\mathrm{S}}}{I_{\mathrm{P}}}\right)(1 - e^{-I_{\mathrm{P}}/P_{\mathrm{S}}})^K \\
&\quad + \sum_{k=1}^{K} \binom{K}{k} (-1)^{k+1} \left(-e^{-\left(\frac{I_{\mathrm{P}}}{P_{\mathrm{S}}}\right)} \ln\left(\frac{I_{\mathrm{P}}}{P_{\mathrm{S}}}\right) + \mathrm{Ei}(-kI_{\mathrm{P}}/P_{\mathrm{S}})\right).
\end{aligned} \tag{55}$$

We next derive $\mathbb{E}\{\ln X_2\}$ as

$$\begin{aligned}
&\mathbb{E}\{\ln X_2\} \\
&= \mathbb{E}_{Y_1}\left\{\mathbb{E}_{\hat{Z}_1}\left\{\ln\left(\frac{1}{KN_{\mathrm{P}}}P_{\mathrm{P}}Y_1 + (1-\sigma^2)\min\left\{\frac{I_{\mathrm{P}}}{\hat{Z}_1}, P_{\mathrm{S}}\right\} + 1\right)\right\}\right\} \\
&= \mathbb{E}_{Y_1}\left\{\int_0^{\infty} \ln\left(\frac{1}{KN_{\mathrm{P}}}P_{\mathrm{P}}Y_1 + (1-\sigma^2)\min\left\{\frac{I_{\mathrm{P}}}{x}, P_{\mathrm{S}}\right\} + 1\right) \right. \\
&\qquad \left. \times f_{\hat{Z}_1}(x)dx\right\} \\
&= F_{\hat{Z}_1}\left(\frac{I_{\mathrm{P}}}{P_{\mathrm{S}}}\right) \\
&\quad \times \int_0^{\infty} \ln\left(\frac{1}{KN_{\mathrm{P}}}P_{\mathrm{P}}y + 1 + (1-\sigma^2)P_{\mathrm{S}}\right) f_{Y_1}(y)dy \\
&\quad + \int_0^{\infty}\int_{\frac{I_{\mathrm{P}}}{P_{\mathrm{S}}}}^{\infty} \ln\left(\frac{1}{KN_{\mathrm{P}}}P_{\mathrm{P}}y + 1 + (1-\sigma^2)\frac{I_{\mathrm{P}}}{x}\right) f_{\hat{Z}_1}(x) f_{Y_1}(y)dxdy
\end{aligned} \tag{56}$$

where $f_{Y_1}(y)$ is the PDF of Y_1, which is given by

$$\begin{aligned}
f_{Y_1}(y) &= \int_0^{\infty} \frac{1}{t} f_{\Upsilon_1}\left(\frac{y}{t}\right) f_{\xi_2}(t)dt \\
&= \frac{2y^{(N_{\mathrm{P}}+K)/2-1} K_{N_{\mathrm{P}}-K}(2\sqrt{y})}{(N_{\mathrm{P}}-1)!(K-1)!}.
\end{aligned} \tag{57}$$

Based on (55) and (56), Δ_2 can be obtained.

REFERENCES

[1] T. L. Marzetta, "Noncooperative cellular wireless with unlimited numbers of base station antennas," *IEEE Trans. Wireless Commun.*, vol. 9, no. 11, pp. 3590–3600, Nov. 2010.

[2] E. G. Larsson, F. Tufvesson, O. Edfors, and T. L. Marzetta, "Massive MIMO for next generation wireless systems," *IEEE Commun. Mag.*, vol. 52, no. 2, pp. 186–195, Feb. 2014.

[3] H. Wang, P. Pan, L. Shen, and Z. Zhao, "On the pair-wise error probability of a multi-cell MIMO uplink system with pilot contamination," *IEEE Trans. Wireless Commun.*, vol. 13, no. 10, pp. 5797–5811, Oct. 2014.

[4] J. Zhu, R. Schober, and V. K. Bhargava, "Secure transmission in multicell massive MIMO systems," *IEEE Trans. Wireless Commun.*, vol. 13, no. 9, pp. 4766–4781, Sep. 2014.

[5] H. Yang and T. L. Marzetta, "Performance of conjugate and zero-forcing beamforming in large-scale antenna systems," *IEEE J. Sel. Areas Commun.*, vol. 31, no. 2, pp. 172–179, Feb. 2013.

[6] S. Haykin, "Cognitive radio: Brain-empowered wireless communications," *IEEE J. Sel. Areas Commun.*, vol. 23, no. 2, pp. 201–220, Feb. 2005.
[7] L. Sboui, Z. Rezki, and M.-S. Alouini, "A unified framework for the ergodic capacity of spectrum sharing cognitive radio systems," *IEEE Trans. Wireless Commun.*, vol. 12, no. 2, pp. 877–887, Feb. 2013.
[8] K. J. Kim, L. Wang, T. Q. Duong, M. Elkashlan, and H. V. Poor, "Cognitive single carrier systems: Joint impact of multiple licensed transceivers," *IEEE Trans. Wireless Commun.*, vol. 13, no. 12, pp. 6741–6755, Dec. 2014.
[9] A. Goldsmith, S. A. Jafar, I. Maric, and S. Srinivasa, "Breaking spectrum gridlock with cognitive radios: An information theoretic perspective," *Proc. IEEE*, vol. 97, no. 5, pp. 894–914, May 2009.
[10] H. A. Suraweera, P. J. Smith, and M. Shafi, "Capacity limits and performance analysis of cognitive radio with imperfect channel knowledge," *IEEE Trans. Veh. Technol.*, vol. 59, no. 4, pp. 1811–1822, May 2010.
[11] M. Filippou, D. Gesbert, and H. Yin, "Decontaminating pilots in cognitive massive MIMO networks," in *Proc. Int. Symp. Wireless Commun. Syst.*, Aug. 2012, pp. 816–820.
[12] B. Kouassi, I. Ghauri, and L. Deneire, "Reciprocity-based cognitive transmissions using a MU massive MIMO approach," in *Proc. IEEE ICC*, Budapest, Hungary, 2013, pp. 2738–2742.
[13] I. S. Gradshteyn and I. M. Ryzhik, *Table of Integrals, Series and Products*, 7th ed. San Diego, CA, USA: Academic, 2007.
[14] H. Shin and M. Z. Win, "MIMO diversity in the presence of double scattering," *IEEE Trans. Inf. Theory*, vol. 54, no. 7, pp. 2976–2996, Jul. 2008.
[15] S. Jin, M. R. McKay, C. Zhong, and K.-K. Wong, "Ergodic capacity analysis of amplify-and-forward MIMO dual-hop systems," *IEEE Trans. Inf. Theory*, vol. 56, no. 5, pp. 2204–2224, May 2010.
[16] P. Hesami and J. N. Laneman, "Limiting behavior of receive antennae selection," in *Proc. 45th Annu. CISS*, Baltimore, MD, USA, Mar. 2011, pp. 1–6.
[17] H. Q. Ngo, E. G. Larsson, and T. L. Marzetta, "Energy and spectral efficiency of very large multiuser MIMO systems," *IEEE Trans. Commun.*, vol. 61, no. 4, pp. 1436–1449, Apr. 2013.
[18] E. Bjornson, L. Sanguinetti, J. Hoydis, and M. Debbah, "Designing multiuser MIMO for energy efficiency: When is massive MIMO the answer?" in *Pro. IEEE WCNC*, 2014, pp. 242–247.
[19] B. Nosrat-Makouei, J. G. Andrews, and R. W. Heath, "MIMO interference alignment over correlated channels with imperfect CSI," *IEEE Trans. Signal Process.*, vol. 59, no. 6, pp. 2783–2794, Jun. 2011.
[20] F. Rusek *et al.*, "Scaling up MIMO: Opportunities and challenges with very large arrays," *IEEE Signal Process. Mag.*, vol. 30, no. 1, pp. 40–60, Jan. 2013.
[21] E. Björnson, J. Hoydis, M. Kountouris, and M. Debbah, "Massive MIMO systems with non-ideal hardware: Energy efficiency, estimation, and capacity limits," *IEEE Trans. Inf. Theory*, vol. 60, no. 11, pp. 7112–7139, Nov. 2014.
[22] D. B. da Costa and S. Aissa, "Cooperative dual-hop relaying systems with beamforming over Nakagami-m fading channels," *IEEE Trans. Wireless Commun.*, vol. 8, no. 8, pp. 3950–3954, Aug. 2009.
[23] H. Q. Ngo, M. Matthaiou, T. Q. Duong, and E. G. Larsson, "Uplink performance analysis of multicell MU-SIMO systems with ZF receivers," *IEEE Trans. Veh. Technol.*, vol. 62, no. 9, pp. 4471–4483, Nov. 2013.
[24] M. Abramowitz and I. A. Stegun, *Handbook of Mathematical Functions With Formulas, Graphs, and Mathematical Tables*, 9th ed. New York, NY, USA: Dover, 1970.

Lifeng Wang received the M.S. degree in electronic engineering from the University of Electronic Science and Technology of China, Chengdu, China, in 2012, and the Ph.D. degree in electronic engineering from Queen Mary University of London, London, U.K., in 2015.

He is currently a Research Associate with the Department of Electronic and Electrical Engineering, University College London, London. His research interests include millimeter-wave communications, Massive multiple input multiple output, heterogeneous networks, cognitive radio, physical layer security, and wireless energy harvesting.

Hien Quoc Ngo (S'12) received the B.S. degree in electrical engineering from Ho Chi Minh City University of Technology, Ho Chi Minh, Vietnam, in 2007, the M.S. degree in electronics and radio engineering from Kyung Hee University, Seoul, Korea, in 2010, and the Ph.D. degree in communication systems from Linköping University (LiU), Linköping, Sweden, in 2015.

From May to December 2014, he visited Bell Laboratories, Murray Hill, NJ, USA. He is currently a Researcher of the Division for Communication Systems with the Department of Electrical Engineering (ISY), LiU. His research interests include Massive (large-scale) multiple-input–multiple-output (MIMO) systems and cooperative communications.

Dr. Ngo has been a member of technical program committees for several IEEE conferences such as ICC, GLOBECOM, WCSP, ISWCS, ATC, and ComManTel. He was an IEEE Communications Letters Exemplary Reviewer in 2014. He was a recipient of the Stephen O. Rice Prize in Communications Theory in 2015 for work on massive MIMO systems and the IEEE Sweden VT-COM-IT Joint Chapter Best Student Journal Paper Award in 2015.

Maged Elkashlan (M'06) received the Ph.D. degree in electrical engineering from The University of British Columbia, Vancouver, BC, Canada, in 2006.

From 2006 to 2007, he was with the Laboratory for Advanced Networking, The University of British Columbia. From 2007 to 2011, he was with the Wireless and Networking Technologies Laboratory, Commonwealth Scientific and Industrial Research Organization, Dickson, Australia. During this time, he held an adjunct appointment with the University of Technology Sydney, Ultimo, Australia. In 2011, he joined the School of Electronic Engineering and Computer Science at Queen Mary University of London, London, U.K., as an Assistant Professor. He also holds visiting faculty appointments with the University of New South Wales, Sydney, Australia, and Beijing University of Posts and Telecommunications, Beijing, China. His research interests fall into the broad areas of communication theory, wireless communications, and statistical signal processing for distributed data processing, heterogeneous networks, cognitive radio, and security.

Dr. Elkashlan currently serves as an Editor of the IEEE TRANSACTIONS ON WIRELESS COMMUNICATIONS, the IEEE TRANSACTIONS ON VEHICULAR TECHNOLOGY, and the IEEE Communications Letters. He also serves as a Lead Guest Editor for the special issue on "Green Media: The Future of Wireless Multimedia Networks" of the IEEE Wireless Communications Magazine, a Lead Guest Editor for the special issue on "Millimeter Wave Communications for 5G" of the IEEE Communications Magazine, a Guest Editor for the special issue on "Energy Harvesting Communications" of the IEEE Communications Magazine, and a Guest Editor for the special issue on "Location Awareness for Radios and Networks" of the IEEE Journal on Selected Areas in Communications. He was a recipient of the Best Paper Award at the IEEE Vehicular Technology Conference (VTC-Spring) in 2013, the IEEE International Conference on Communications in 2014, and the International Conference on Communications and Networking in China (CHINACOM) in 2014. He was also a recipient of the Exemplary Reviewer Certificate of the IEEE Communications Letters in 2012.

Trung Q. Duong (S'05–M'12–SM'13) received the Ph.D. degree in telecommunications systems from Blekinge Institute of Technology, Karlskrona, Sweden, in 2012.

Since 2013, he has been a Lecturer (Assistant Professor) with Queen's University Belfast, Belfast, U.K. He has authored or coauthored 170 technical papers published in scientific journals and presented at international conferences. His current research interests include cooperative communications, cognitive radio networks, physical layer security, massive multiple input multiple output, cross-layer design, millimeter-wave communications, and localization for radios and networks.

Dr. Duong currently serves as an Editor of the IEEE Communications Letters, IET Communications, and Wiley Transactions on Emerging Telecommunications Technologies. He has also served as the Guest Editor of the special issue on some major journals, including the IEEE Journal on Selected Areas in Communications, IET Communications, the IEEE Wireless Communications Magazine, the IEEE Communications Magazine, EURASIP Journal on Wireless Communications and Networking, and EURASIP Journal on Advances in Signal Processing. He was a recipient of the Best Paper Award at the IEEE Vehicular Technology Conference (VTC-Spring) in 2013 and the IEEE International Conference on Communications in 2014.

Kai-Kit Wong (M'01–SM'08) received the B.Eng., M.Phil., and Ph.D. degrees from The Hong Kong University of Science and Technology, Kowloon, Hong Kong, in 1996, 1998, and 2001, respectively, all in electrical and electronic engineering.

He is currently a Reader in Wireless Communications in the Department of Electronic and Electrical Engineering, University College London, London, U.K.

Dr. Wong is a Fellow of The Institution of Engineering and Technology. He is a Senior Editor of the IEEE Communications Letters and is on the editorial board of the IEEE Wireless Communications Letters, IEEE ComSoc/KICS Journal of Communications and Networks, IET Communications, and Physical Communications. He served as an Editor of the IEEE TRANSACTIONS ON WIRELESS COMMUNICATIONS from 2005 to 2011 and the IEEE Signal Processing Letters from 2009 to 2012.